Supporting Information

Investigating the Structure–Stability Relationship in Bridging Isomers of Bistetrazoles

Sarika Venugopal, Bhargav Kolekar, Rahul V Pinjari,* Anuj A Vargeese*

1. Materials and methods

1.1 Materials

The required reagents and solvents were purchased from Tokyo Chemical Industry, Spectrochem, Nice Chemicals, or Qualigens-Thermo Fisher Scientific, and used without further purification.

NMR spectra were recorded on a JEOL 500 MHz NMR Spectrometer with dimethyl sulfoxide DMSO-d_6 as solvent. Chemical shift values are reported in δ units (parts per million) relative to tetramethylsilane (TMS) as an internal standard for ^{1}H and ^{13}C and liquid ammonia as an internal standard for ^{15}N. IR spectra were recorded on a PerkinElmer Spectrum Two FT-IR spectrometer and the values are reported in cm^{-1}.

1.2 Synthesis

1.2.1 Synthesis of 5,5'-Bis-1H-tetrazole (1):[1]
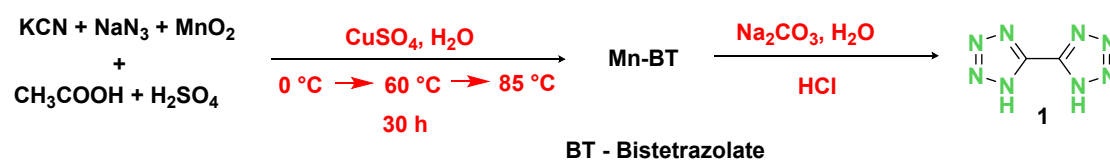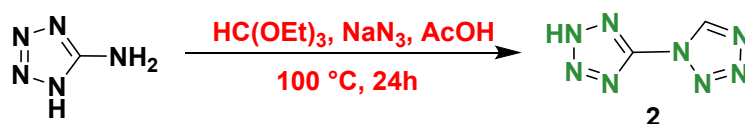

Scheme. S1 Synthesis scheme of compound (**1**)

Sodium azide (1.1979g, 18 mmol) was added to a solution of potassium cyanide (1.2g, 18 mmol) in 6 ml of water under ice-bath condition. Manganese dioxide (1.0015g, 11.52 mmol) was added at the same temperature and stirred for one hour. A mixture of 1 ml sulphuric acid (98%), 1.5 ml glacial acetic acid, copper sulphate pentahydrate (0.0292g, 0.12 mmol), and 2 ml of water was prepared and stirred in an ice-bath for one hour. This solution was slowly added to the first solution and allowed to react for one hour. Then the reaction mixture was refluxed at 60 °C for 15 hours. Subsequently, the temperature was raised to 85 °C, and the reaction was performed for an additional 15 hours. The obtained grey-solid (Mn-bistetrazolate) was filtered. Next, sodium carbonate (0.3592 g, 3.39 mmol) was added to a

slurry consisting of manganese bistetrazolate (0.5994 g, 3.14 mmol) in 5 ml of water and then the mixture was heated at 80 °C for 30 minutes. The obtained blue-coloured solution was filtered and excess amount of hydrochloric acid was added to the solution until a white precipitate is formed. After that, the precipitate was dissolved by boiling the solution and the solution was cooled overnight to give crystals of 5,5'-Bis-1H-tetrazole. ^{1}H NMR (500 MHz, DMSO-d$_6$) δ: 8.012 (br. s, 2H); ^{13}C NMR (125 MHz, DMSO-d$_6$) δ: 148.118; ^{15}N NMR (50 MHz, DMSO-d$_6$), δ: 360.696, 288.426; IR (UATR): $\bar{v}$ = 3400-3600, 2800-3200, 3033, 2448, 2345, 1851, 1601, 1535, 1434, 1331, 1267, 1164, 1111, 1051, 966, 872, 730, 610 cm^{-1}; HRMS (ESI-TOF): calculated for C$_2$HN$_8^-$ [M-H]$^-$:137.033, found: 137.0325.

*1.2.2 Synthesis of 5-(Tetrazol-1-yl)-2H-tetrazole (**2**):*[2]

Scheme. S2 Synthesis scheme of compound (**2**)

Glacial acetic acid (11.8 mL) was added dropwise to a mixture of 5-aminotetrazole (2 g, 23.5 mmol), sodium azide (1.834 g, 28.2 mmol) and triethyl orthoformate (5.226 g, 35.3 mmol, 5.9 mL) at 60 °C under vigorous stirring. After 24 h under reflux condition (90 °C), the clear solution obtained was cooled to room temperature and stirred with hydrochloric acid (2M, 14 mL). After 1 hour, the solvent was completely evaporated under vacuum and the residue was suspended in toluene. Then the solvent was evaporated again to remove traces of acetic acid. This procedure was repeated and the dry residue was dissolved in hydrochloric acid

(0.5M, 47 mL), extracted with ethyl acetate and the combined organic phases were dried over sodium sulphate. After evaporation of the solvent under vacuum, the residue was washed well with diethyl ether to yield anhydrous 5-(tetrazol-1-yl)-2H-tetrazole (**1**) as a white powder (0.6430 g, 19.8 %). ^{1}H NMR (500 MHz, DMSO-d$_6$) δ: 10.19 (s, 1H); ^{13}C NMR (125 MHz, DMSO-d$_6$) δ: 155.40, 144.21; ^{15}N NMR (50 MHz, DMSO-d$_6$), δ: 390.008, 357.94, 341.78, 325.63, 291.54, 223.25; IR (UATR): $\bar{v}$ = 3162, 3128, 3035, 2973, 2630, 2499, 1820, 1702, 1697, 1656, 1578, 1454, 1382, 1370, 1271, 1207, 1176, 1146, 1113, 1083, 1019, 991, 957, 910, 890, 871, 742, 647 cm^{-1}; HRMS (ESI-TOF): calculated for C$_2$H$_2$N$_7^-$ [M-H]$^-$:137.033, found: 137.0335.

1.3 Kinetic Analysis

In Vyazovkin's method[3], for a set of 'n' experiments are conducted at different heating rates, the apparent activation energy can be determined at any given value of α by identifying the value of E_α for which the given function, Eq. (2), is a minimum. Here, β represents the heating rate, i and j are the set of experiments performed under different heating rates, and n is the total number of experiments performed. The third-degree approximation shown in Eq. (4)[4] was used to calculate the integral in Eq. (3). MATLAB R2020a was used to perform the kinetic computations.

$$\sum_{i}^{n}\sum_{j \neq i}^{n}\left[I\left(E_\alpha, T_{\alpha,i}\right)\beta_j\right]/\left[I\left(E_\alpha, T_{\alpha,j}\right)\beta_i\right] = min$$

.... (2)

Where,
$$I(E,T) = \int_{0}^{T} e^{-\left(\frac{E}{RT}\right)} dT$$

.... (3)

$$f(x) = \frac{e^{-x}}{x} \times \frac{x^2 + 10x + 18}{x^3 + 12x^2 + 36x + 24}$$

.... (4)

Where,
$$x = \frac{E}{RT} \quad \text{and} \quad I(E,T) = \frac{E}{R}f(x)$$

.... (5)

2. Characterization data:
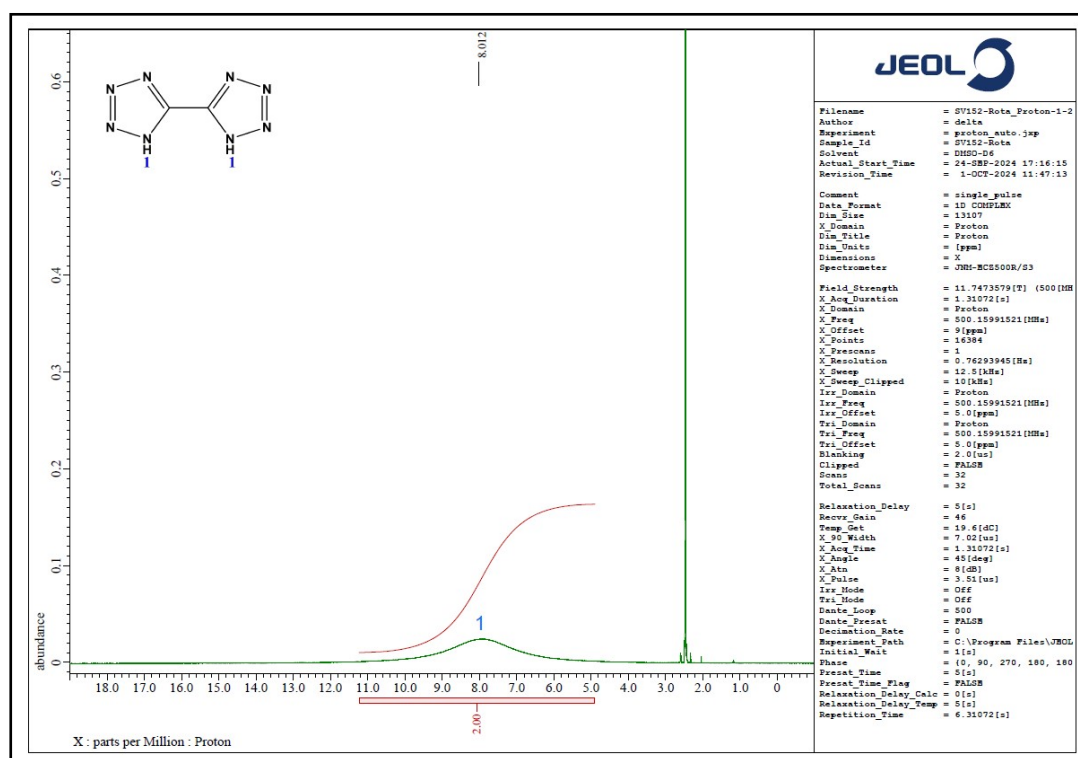
Fig. S1 ^{1}H NMR spectrum of compound **1** in DMSO-d$_6$
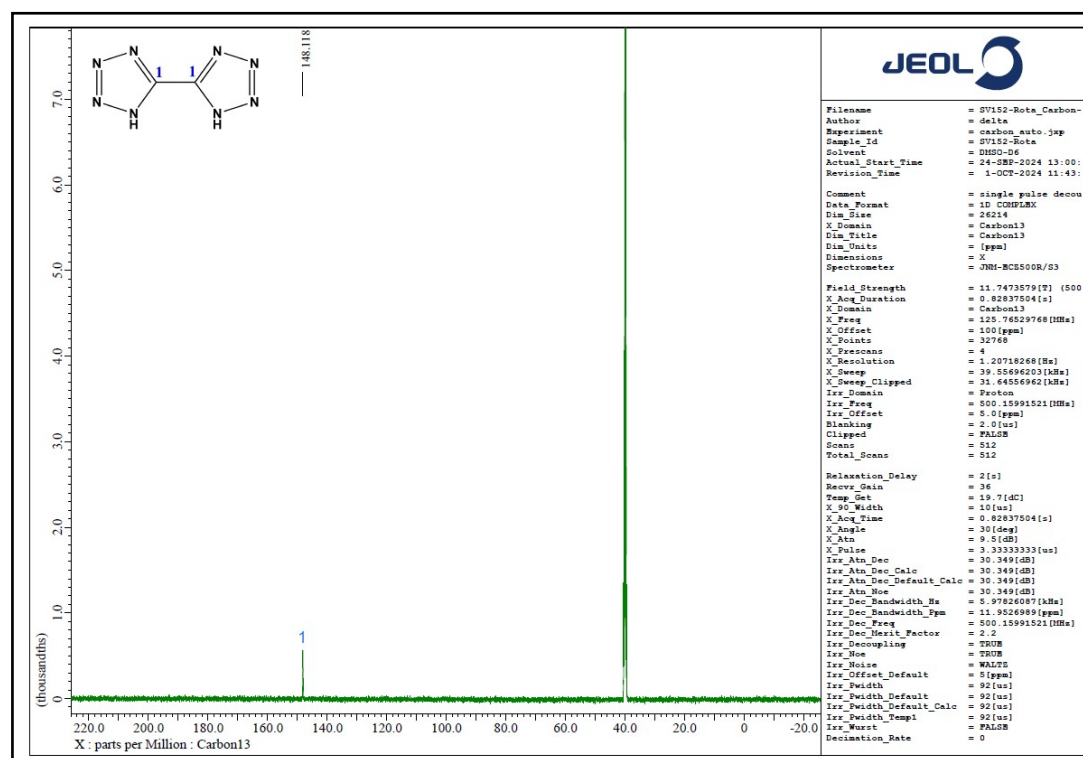
Fig. S2 ^{13}C NMR spectrum of compound **1** in DMSO-d$_6$
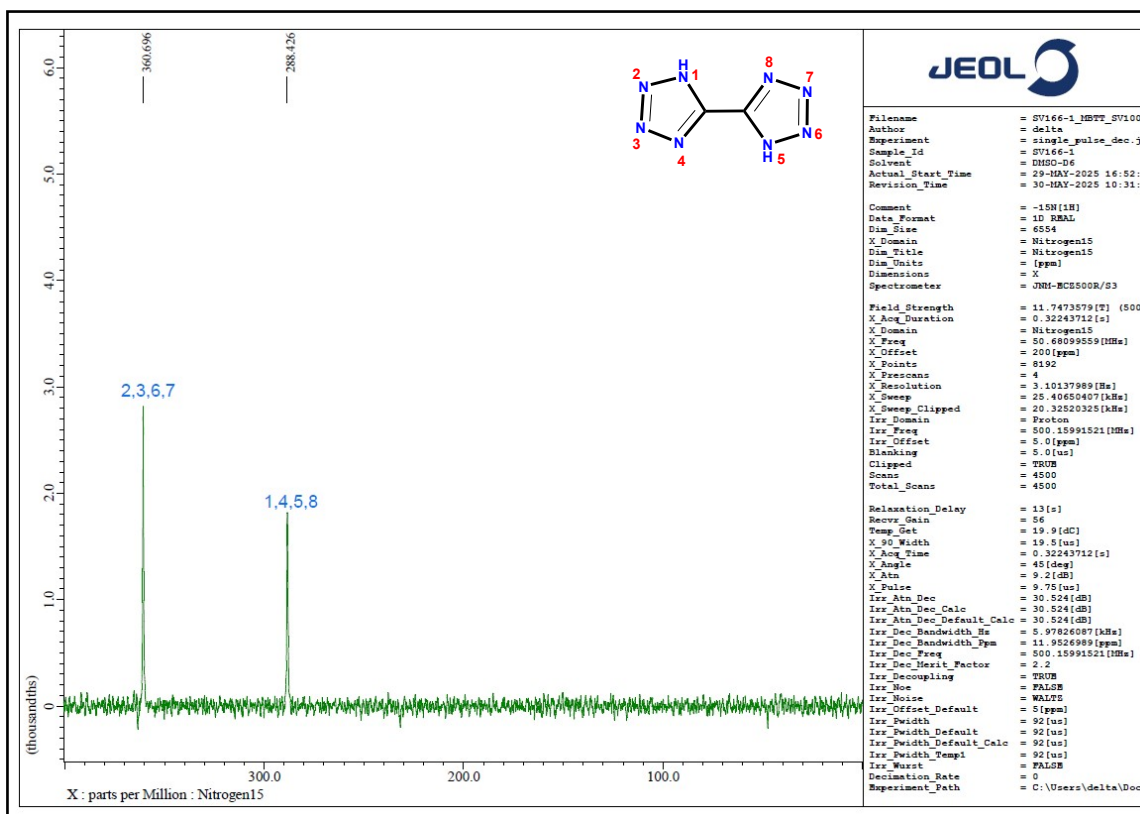
Fig. S3 ^{15}N NMR spectrum of compound **1** in DMSO-d$_6$
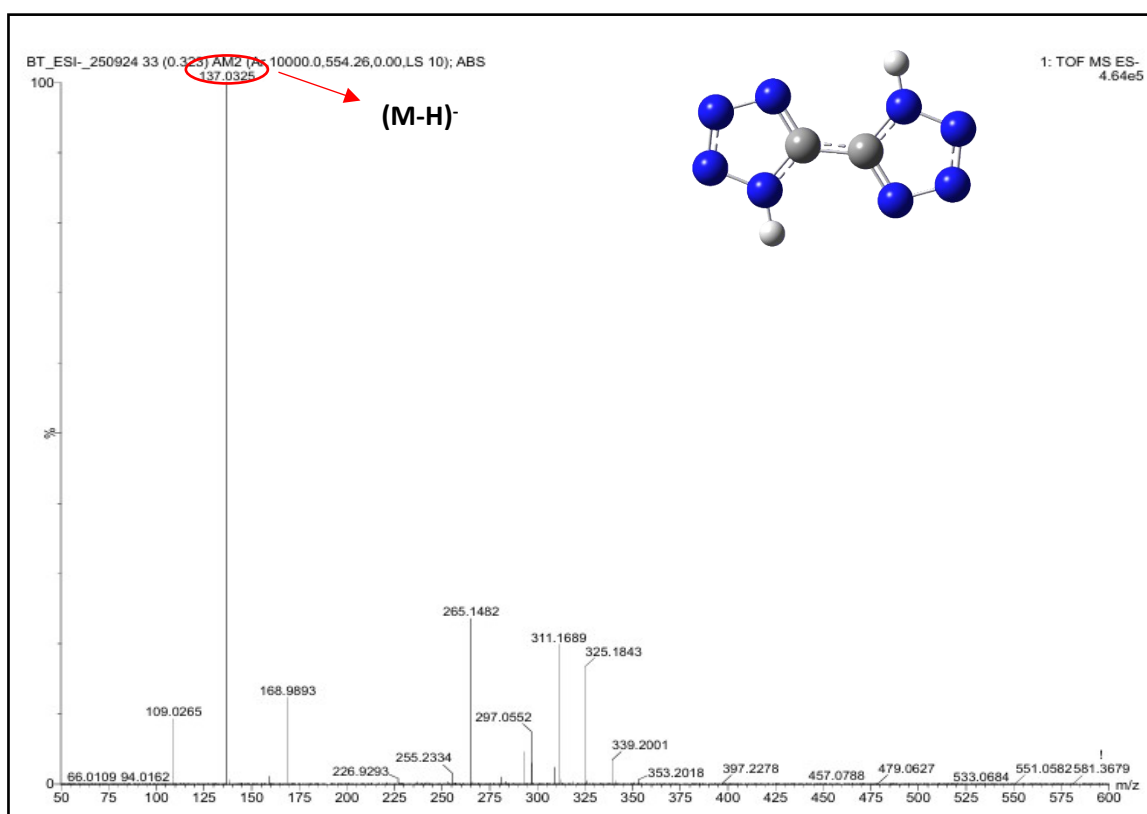
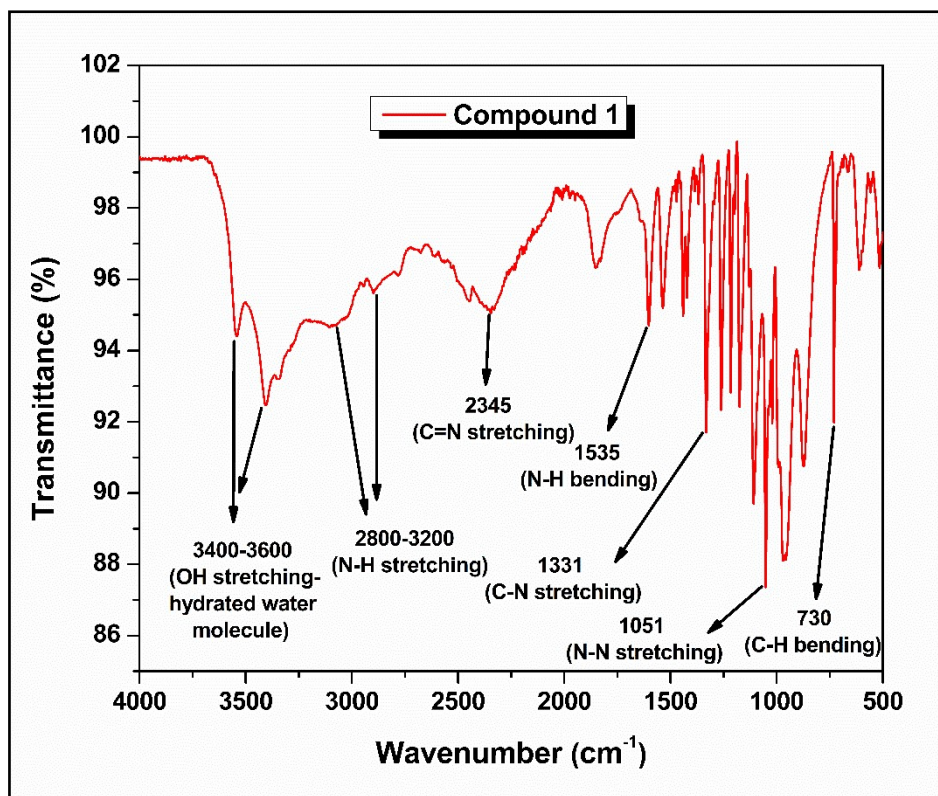**Fig. S4** HRMS spectrum of compound **1**

Fig. S5 IR spectrum of compound **1**
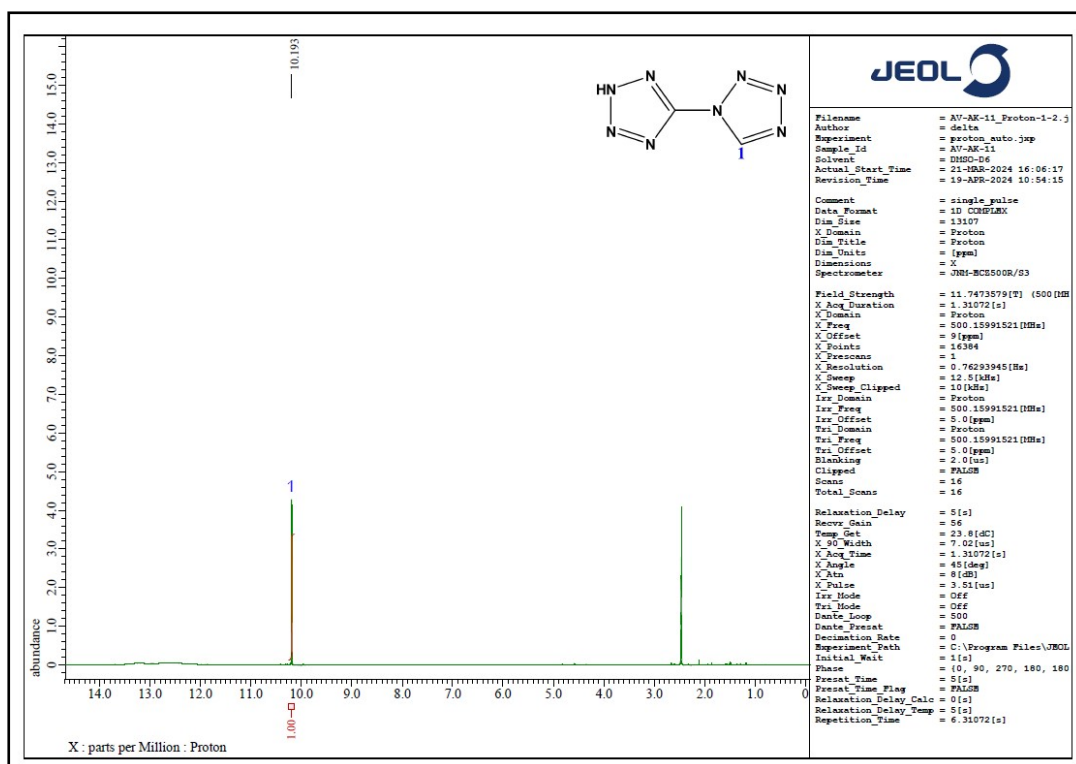
Fig. S6 ¹H NMR spectrum of compound **2** in DMSO-d₆
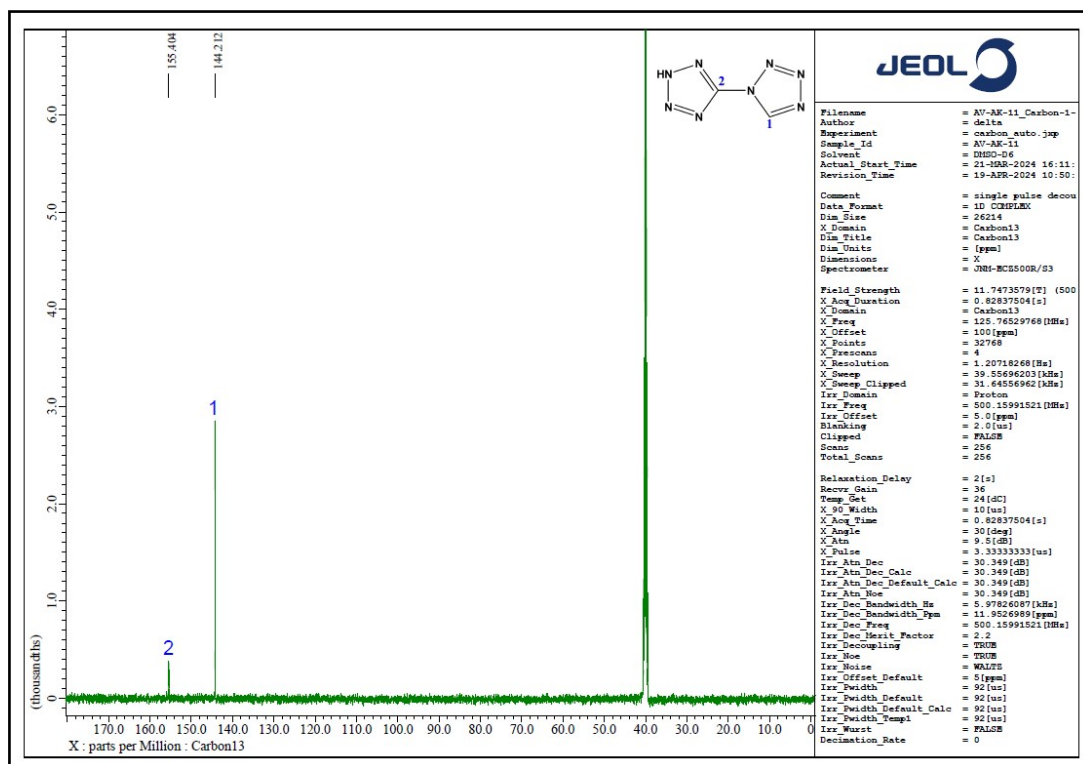
Fig. S7 ^{13}C NMR spectrum of compound **2** in DMSO-d$_6$
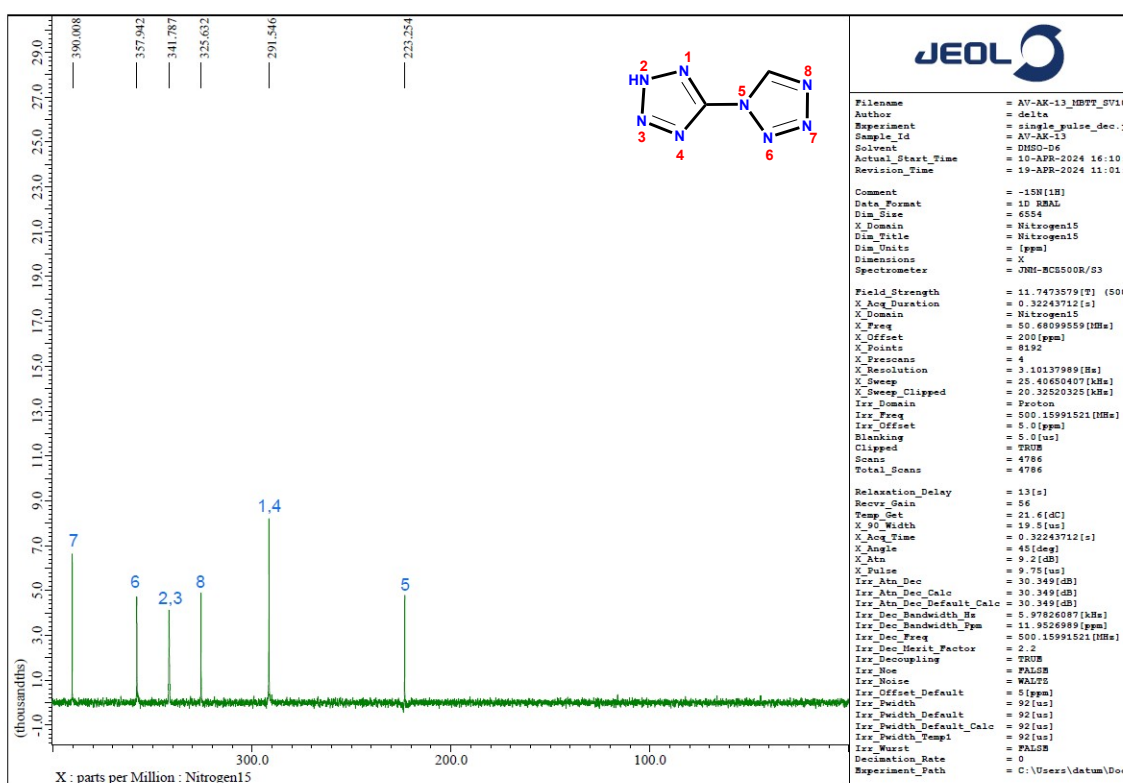
Fig. S8 ^{15}N NMR spectrum of compound **2** in DMSO-d$_6$
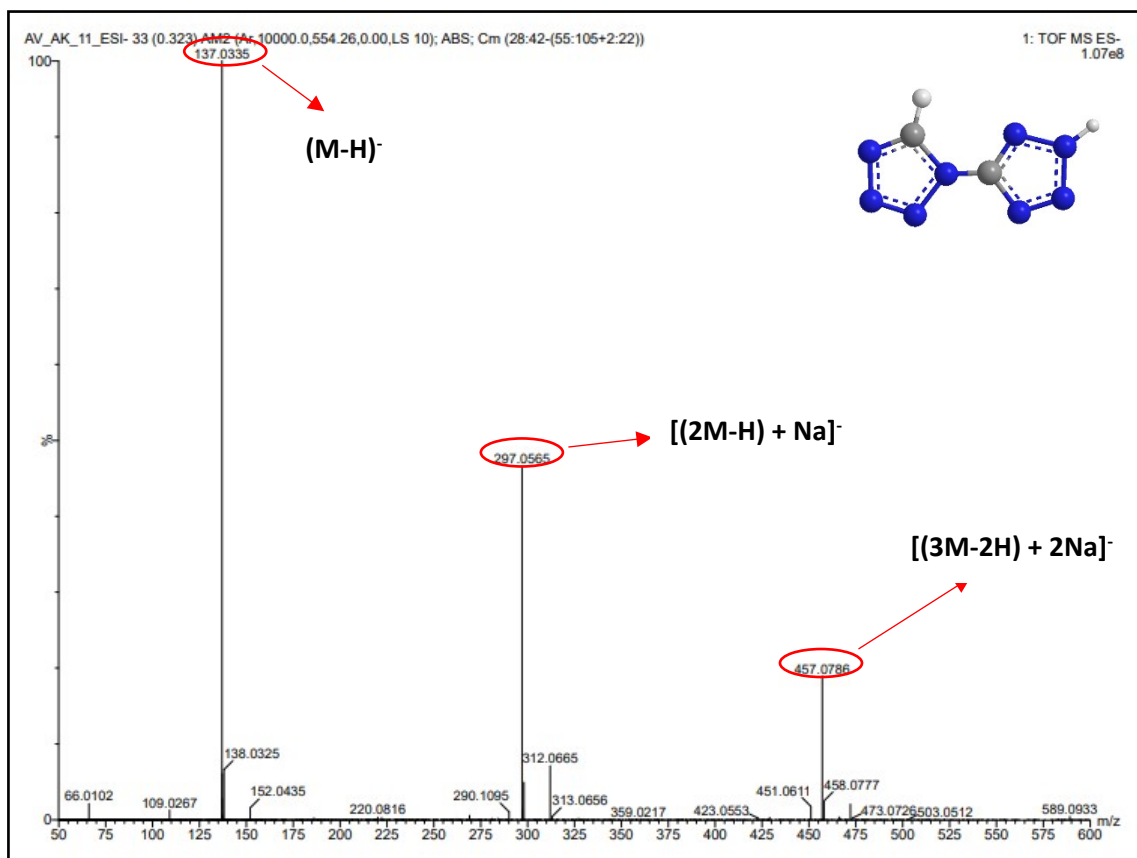
Fig. S9 HRMS spectrum of compound **2**
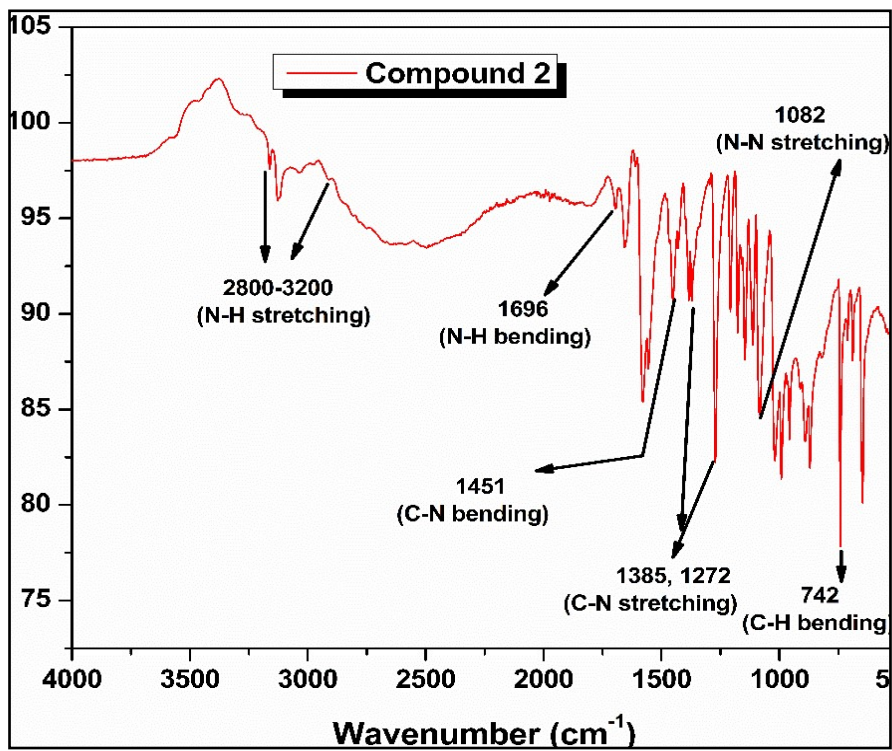
Fig. S10 IR spectrum of compound **2**

3. Thermal analysis data:

Compound	Decomposition					
	Onset temperature (°C)		Peak temperature (°C)		End temperature (°C)	
	TG (DTG)	DSC	TG (DTG)	DSC	TG (DTG)	DSC
1	233	238	259	261	279	292
2	120	135	145	150	160	167

Table. S1 Thermal analysis data of compounds **1** and **2**

4. Kinetic analysis data:
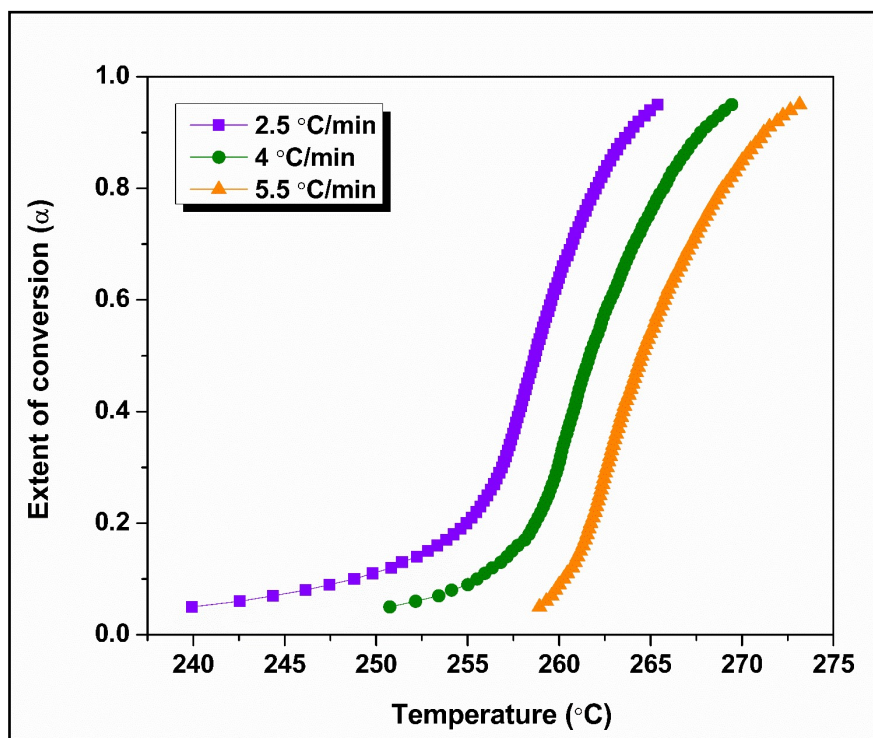
Fig. S11 α-T curves of compound **1** at 2.5, 4, and 5.5 °C/min
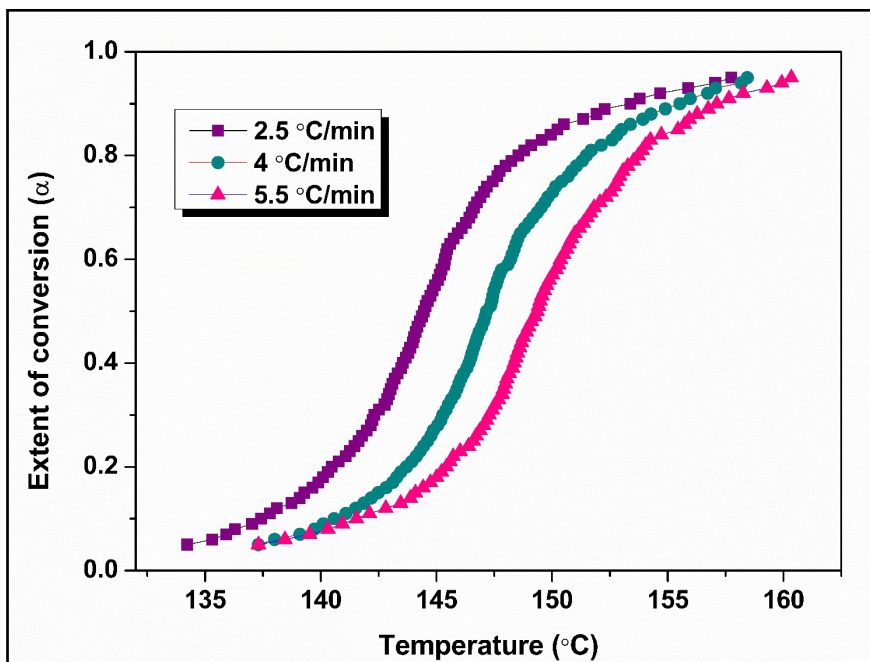
Fig. S12 α-T curves of compound **2** at 2.5, 4, and 5.5 °C/min
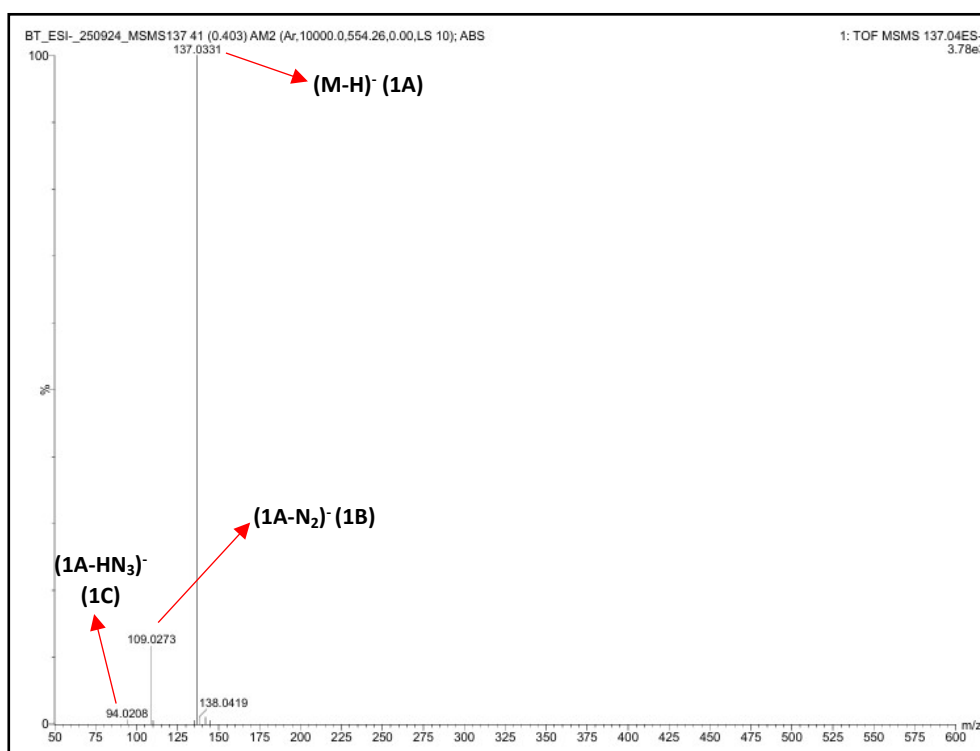
5. MS/MS analysis data

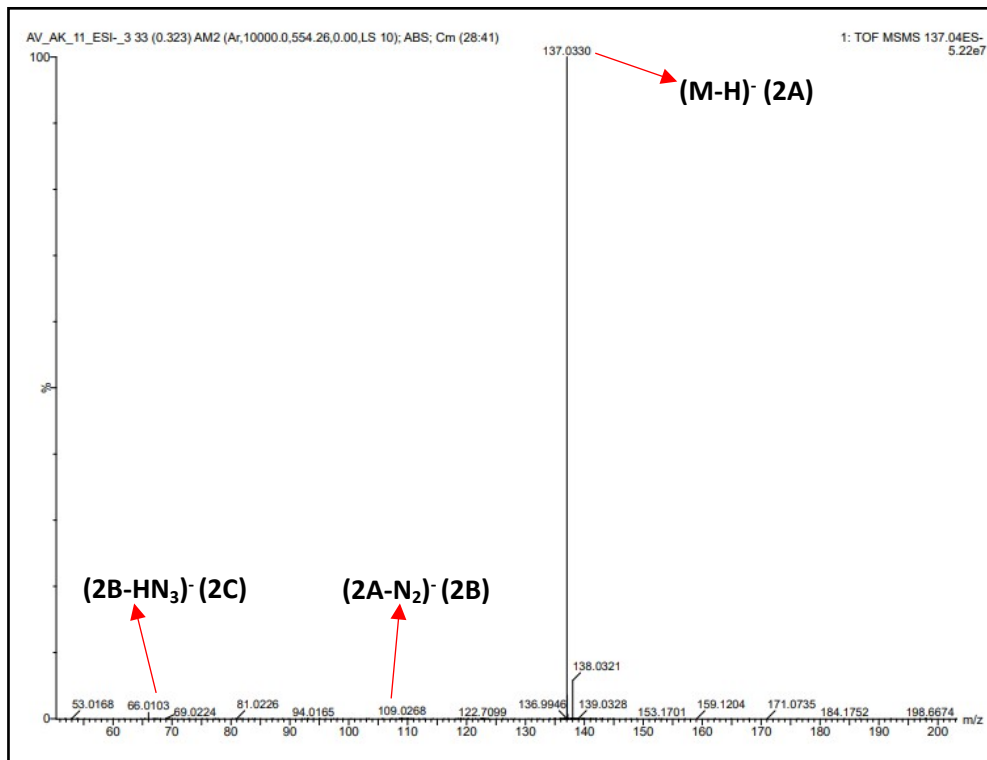**Fig. S13** MS/MS of compound **1** at m/z 137.04[5]

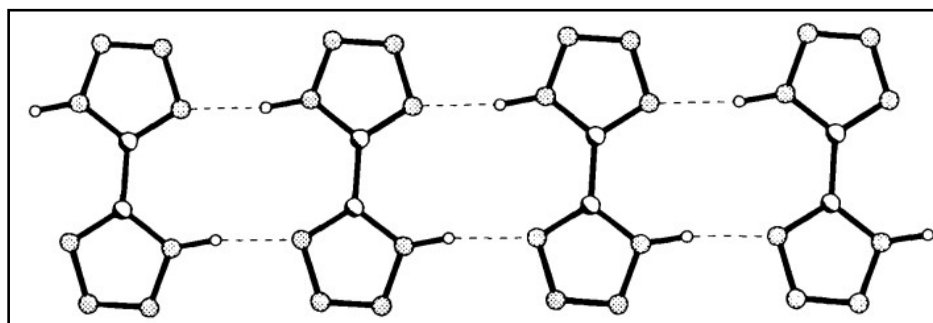

Fig. S14 MS/MS of compound **2** at m/z 137.04

6. Crystal structure

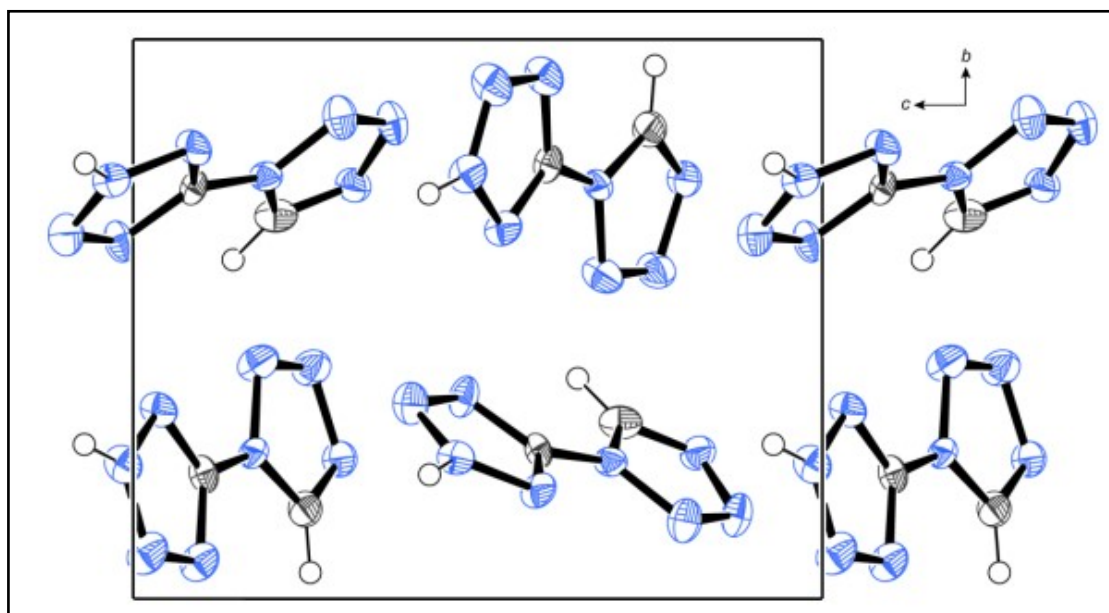**Fig. S15** Molecular packing of Compound **1** with intermolecular hydrogen bonding[6]

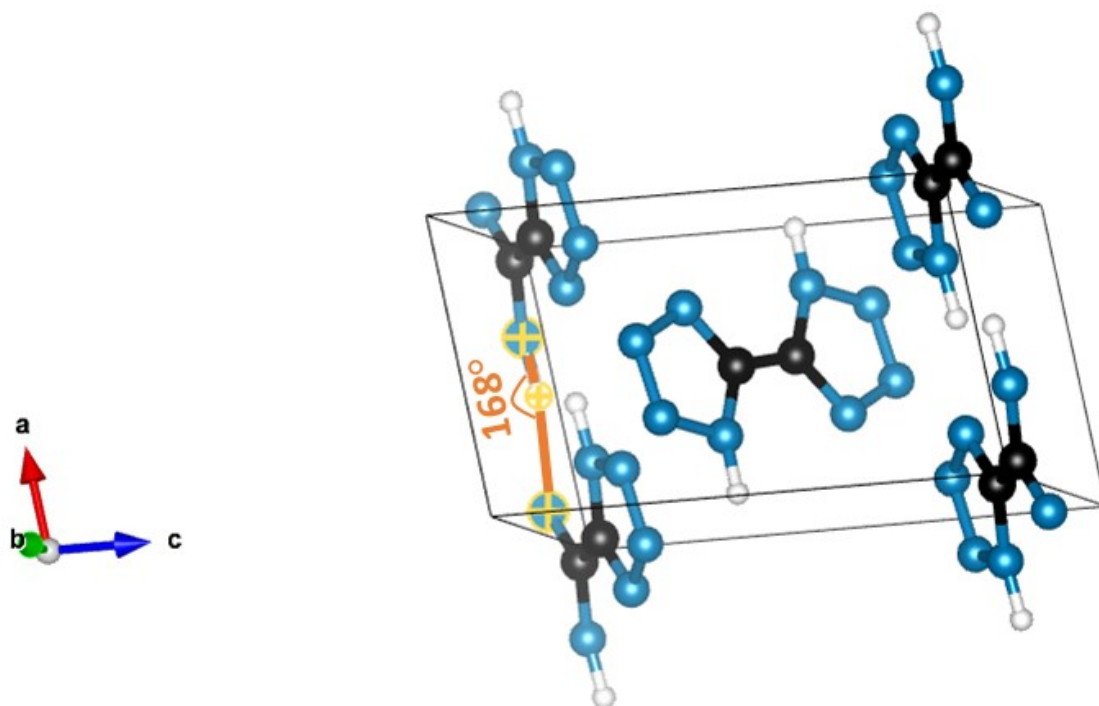**Fig. S16** View on the unit cell of Compound **2** along the inverse a-axis[2]

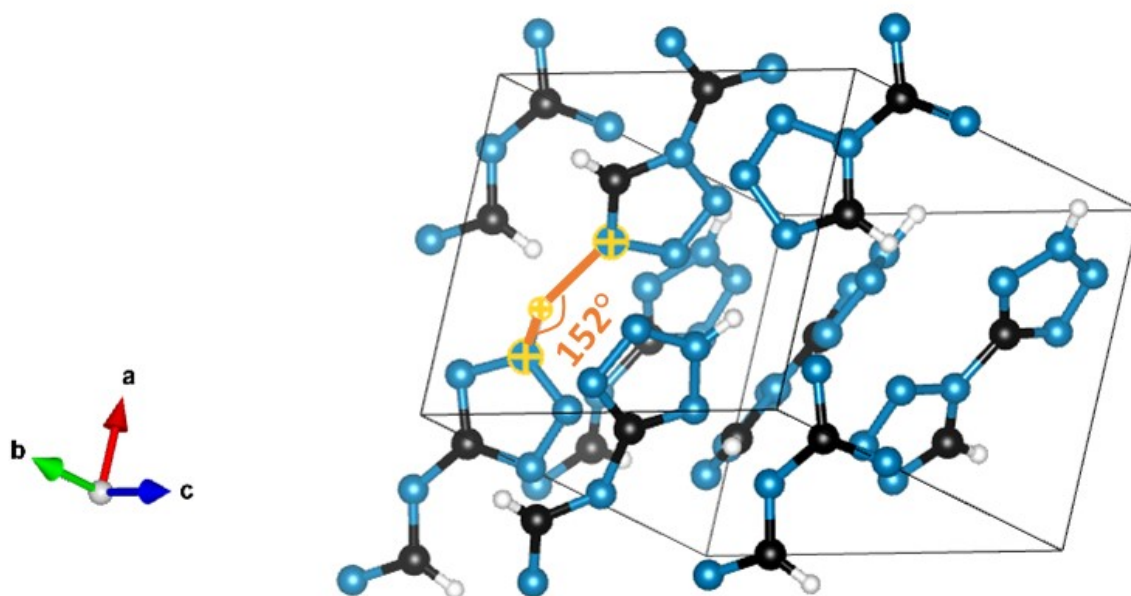**Fig. S17** Dihedral angle of compound **1** measured using Vesta 3 software[7]

Fig. S18 Dihedral angle of compound **2** measured using Vesta 3 software[7]
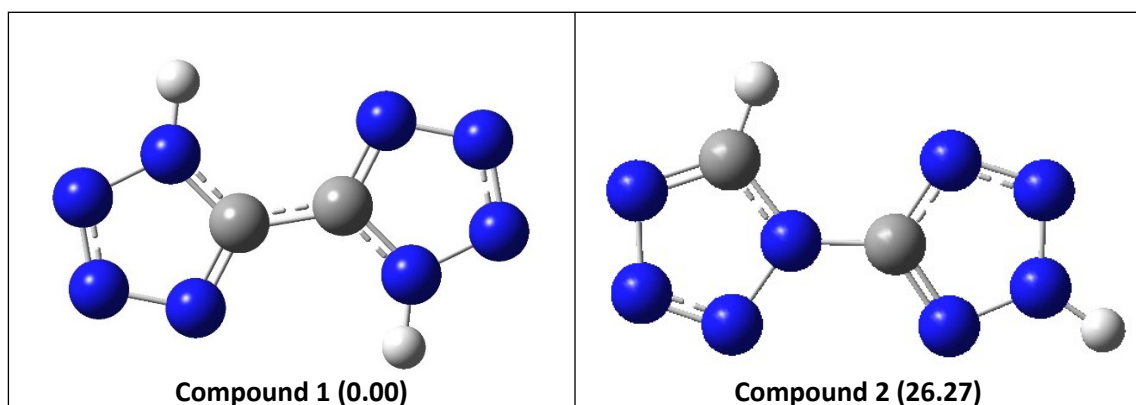
7. Computational Studies

Fig. S19 The optimized geometries of the lowest energy monomers of the compound **1**, and compound **2** (The relative stabilization energy ($\Delta\Delta G_{Rel} = \Delta G_{Molecule} - \Delta G_{Compound-1}$) with respect compound **1** in kJ/mol is given in the bracket)
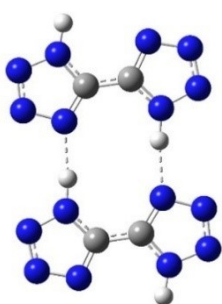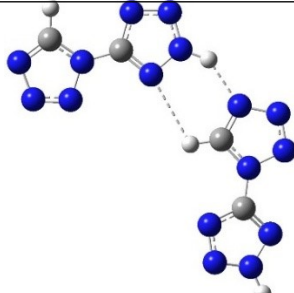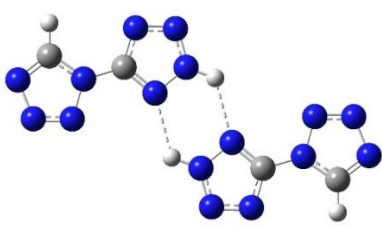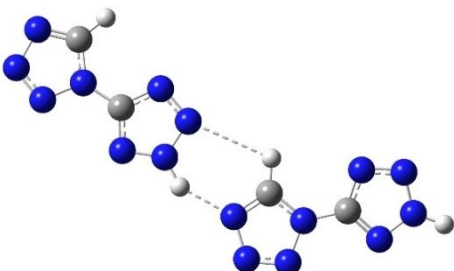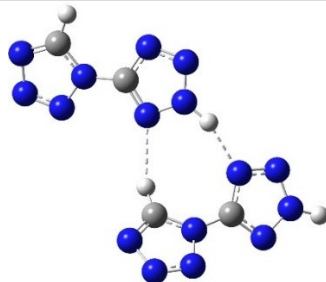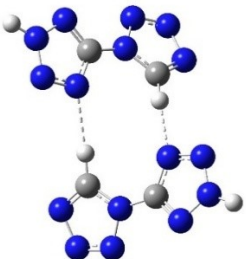
Compound-1-Dimer-1 (-32.76)
A(N-H---N) = 173.786°, d(H---N) = 1.038 Å

Compound-2-Dimer-1 (-6.81)
A(N-H---N) = 143.897° and A(C-H---N) =110.726
d(CH---N) = 1.078 Å and d(NH---N) = 1.032 Å

Compound-2-Dimer-2 (-6.02)
A(N-H---N) = 124.498° and d(NH---N) = 1.020 Å

Compound-2-Dimer-3 (-4.72)
A(N-H---N) = 145.959°and d(C—H) = 1.078 Å
A(C-H---N) = 110.215°and d(H---N) = 1.032 Å

Compound-2-Dimer-4 (4.47)
A(N-H---N) = 158.209°and d(C—H) = 1.080 Å
A(C-H---N) = 152.305°and d(H---N) = 1.029 Å

Compound-2-Dimer-5 (17.57)
A(C-H---N) = 175.755° and d(C—H) = 1.080 Å

Fig. S20 The optimized geometries of the dimers of compound **1** and compound **2**. The dimerization energy ($\Delta\Delta G_{Dimerzation} = \Delta G_{Dimer} - 2*\Delta G_{Monomer}$) with respect to their corresponding monomer in kJ/mol is given in the bracket

TS	uB3LYP-D3/6-311++G(d,p)	uB3LYP-D3/6-311++G(2d,2p)	uM06-2X-D3/6-311++G(d,p)	uM06-2X-D3/6-311++G(2d,2p)
C1_A_TS	103.34	104.89	128.52	130.59
C1_B_TS	180.79	184.47	214.06	218.13
C1_C_TS	177.77	177.06	203.03	203.91
C1_D_TS	257.10	260.90	295.05	299.10
C1_E_TS	296.22	298.36	326.95	329.27
C1_F_TS	339.15	340.95	376.89	379.41
C1_G_TS	290.24	291.09	326.69	327.32

Table. S2 TS energies (in kJ/mol) of the initial degradation steps of compound **1** via different pathways.

Reference

1   Z. Noorpoor and S. Tavangar, Preparation and characterization of Cu based on 5,5'-bistetrazole as a recyclable metal-organic framework and application in synthesis of diaryl ether by the Ullmann coupling reaction, *J Coord Chem*, 2021, **74**, 1651–1662.

2   N. Fischer, D. Izsák, T. M. Klapötke and J. Stierstorfer, The chemistry of 5-(tetrazol-1-yl)-2H-tetrazole: An extensive study of structural and energetic properties, *Chemistry - A European Journal*, 2013, **19**, 8948–8957.

3   S. Vyazovkin, Evaluation of activation energy of thermally stimulated solid-state reactions under arbitrary variation of temperature, *J. Comput. Chem.*, 1997, **18**, 393–402.

4   G. I. ; Senum and Yang. R. T, Rational Approximations of the Integral of the Arrhenius Function, *J. Therm. Anal.* , 1977, **119**, 445–447.

5   S. Venugopal and A. A. Vargeese, Decomposition Mechanism of Alkylidene Bridged Tetrazoles With Different Carbon Chain Lengths, *ChemPhysChem*, DOI:10.1002/cphc.202400943.

6   P. J. Steel, *Heterocyclic tautomerism. XI. Structures of 5,5'-bitetrazole and 1-methyl-5-(2'-pyridyl)tetrazole at 130 K*, 1996, vol. 26.

7   K. Momma and F. Izumi, *VESTA 3* for three-dimensional visualization of crystal, volumetric and morphology data, *J Appl Crystallogr*, 2011, **44**, 1272–1276.